Journal of Contaminant Hydrology 149 (2013) 46–60

Contents lists available at SciVerse ScienceDirect

Journal of Contaminant Hydrology

journal homepage: www.elsevier.com/locate/jconhyd

Scalar dissipation rates in non-conservative transport systems

Nicholas B. Engdahl [a,*], Timothy R. Ginn [b], Graham E. Fogg [a]

[a] Department of Land, Air and Water Resources, University of California, Davis, United States
[b] Department of Civil and Environmental Engineering, University of California, Davis, United States

ARTICLE INFO

Article history:
Received 27 June 2012
Received in revised form 9 March 2013
Accepted 10 March 2013
Available online 26 March 2013

Keywords:
Scalar dissipation rate
Reactive transport
Mixing measures
Mixing

ABSTRACT

This work considers how the inferred mixing state of diffusive and advective–diffusive systems will vary over time when the solute masses are not constant over time. We develop a number of tools that allow the scalar dissipation rate to be used as a mixing measure in these systems without calculating local concentration gradients. The behavior of dissipation rates is investigated for single and multi-component kinetic reactions and a commonly studied equilibrium reaction. The scalar dissipation rate of a tracer experiencing first-order decay can be determined exactly from the decay constant and the dissipation rate of a passive tracer, and the mixing rate of a conservative component is not the superposition of the solute specific mixing rates. We then show how the behavior of the scalar dissipation rate can be determined from a limited subset of an infinite domain. Corrections are derived for constant and time dependent limits of integration the latter is used to approximate dissipation rates in advective–diffusive systems. Several of the corrections exhibit similarities to the previous work on mixing, including non-Fickian mixing. This illustrates the importance of accounting for the effects that reaction systems or limited monitoring areas may have on the inferred mixing state.

1. Introduction

Discrepancies between the predicted and observed behaviors of reactive solutes in groundwater systems often result from differences between laboratory derived rate constants and upscaled, or effective, reaction rates (Battiato et al., 2009; Kapoor et al., 1997; Tartakovsky et al., 2008; Werth et al., 2006). Many of these differences have been attributed to the fact that laboratory estimates of reaction rates are usually based on a well-mixed system but heterogeneities in the flow and transport properties of the subsurface create highly variable solute distributions that are poorly mixed. The persistence of this imperfect mixing over time can cause effective reaction rates to remain well below their laboratory derived values and an accurate representation of mixing becomes a prerequisite for predicting upscaled reaction rates (De Simoni et al., 2007; Le Borgne et al., 2011; Luo et al., 2008).

The physical processes that lead to mixing affect both the internal structure of a plume and the extents of the plume, but it is important to note that mixing and spreading are not describing the same aspects of solute migration. For a passive tracer moving through a groundwater system, the extents of the plume over time are often driven by advective forces that stretch out the plume whereas heterogeneous concentration distributions within the solute plume are attenuated by diffusive or local dispersive processes. There is a complex interaction between all of these processes in heterogeneous environments, and separating the two can be challenging, but understanding the spatio-temporal changes in the mixing state of a plume is a critical research area for improving predictions of reactive transport (Rolle et al., 2009).

The mixing state can be thought of as a measure of how homogeneous the distribution of a solute is within the plume at a given time; this is in contrast to a mixing rate which is the time rate of change of a mixing measure. Physically, the mixing rate quantifies how rapidly the molecules of two or more distinct populations (i.e. combinations of one or more solutes and clean water) that have come into contact with each other

* Corresponding author. Tel.: +530 341 3044.
E-mail address: nbengdahl@ucdavis.edu (N.B. Engdahl).

0169-7722/$ – see front matter © 2013 Elsevier B.V. All rights reserved.
http://dx.doi.org/10.1016/j.jconhyd.2013.03.003

are homogenizing. A well-mixed system is one where the solute concentrations within the plume are essentially uniform but descriptions of the mixing state are, to some extent, independent of the shape of the plume, even though mixing and spreading are inextricably linked. For example, heterogeneous spreading of a plume can enhance the rate of mixing because the elongated plume will have more area for the forces of dispersion and diffusion to work on (Cirpka and Kitanidis, 2000). In other words, mixing can be enhanced by the dilution of a plume and Kitanidis (1994) proposed the dilution index as a quantitative measure of the volume occupied by a solute. The dilution index is calculated from the entropy of the solute distribution, and a mixing rate can be defined from the time rate of change of the entropy (Dentz et al., 2011). This approach is well established and has been used to quantify mixing in a wide variety of passive transport studies but only a recent study by Chiogna et al. (2012) has considered the dilution index in reactive transport systems. The dilution index is not the only approach to quantifying mixing and stochastic hydrology has often modeled the behavior of solute plumes as a linear combination of the mean behavior of the plume and a fluctuation about that mean. This approach is naturally suited to describing mixing because the relative homogeneity of a plume (*i.e.* the mixing state) can be expressed in terms of the variance of the concentration fluctuations (Kapoor and Gelhar, 1994; Miralles-Wilhelm et al., 1997). If there are no deviations from the mean concentration, the solute is internally homogeneous and, by definition, well-mixed. Another approach is to consider the concentration gradients within the solute plume directly (e.g. Le Borgne et al., 2010). This is very similar in principle to the concentration fluctuation approach but these methods have classically been applied to turbulent flows and combustion. Gradient based mixing measures have been used recently to quantify the mixing state and estimate reaction rates in a variety of contaminant hydrology problems including multicomponent reactive transport.

The definition of a well-mixed system does not change when there are multiple solutes because the extent of mixing still describes how uniformly the solutes are distributed but the issue of overlap or segregation must be addressed (e.g. Raje and Kapoor, 2000). By overlap we mean that portions of two or more solute distributions are occupying the same physical space (Cirpka and Kitanidis, 2000). Apparent overlap occurs when upscaled or averaged concentration fields appear to overlap but there is no physical contact and this can have strong effects on effective reaction rates (Kapoor et al., 1997). Since it is an artifact from having incomplete knowledge of the system, we will not consider apparent overlap here and restrict our discussion of overlap to the case of physically co-located solutes. The concepts of mixing and overlapping are often poorly delineated in the literature and are routinely combined into "mixing." This is an important point because stating that two reactive solutes are merely overlapping is insufficient for predicting reaction rates. Identifying overlapping regions provides little, if any, information about the internal distribution of each solute because only their extents have been described (Kapoor et al., 1997). As each solute continues to diffuse and become more efficiently mixed, the distributions of their masses may also be changing due to reactions and this will have an effect on the inferred mixing state (by inferred we mean the mixing state at some time as estimated or calculated from a global mixing measure). Although the total mass of the reaction system is conserved, the mixing state of individual solutes no longer appears conservative because of mass transformations from the reactions. The magnitude of these effects at any location should be proportionate to the local reaction rate or, more precisely, the rate law governing the reaction (e.g. De Simoni et al., 2005, 2007). Conceptually, reactions create local sources and sinks of mass for one solute relative to the others and these changes in mass should affect the mixing state, much like sources and sinks of concentration variance (e.g. Kapoor and Gelhar, 1994); obviously, reactions are not the only possible mechanism that can cause source/sink like behavior. A similar effect can be conceived for the case where we merely have incomplete knowledge of the concentration field. For example, if some portion of the solute mass were to pass beyond the extents of a monitoring network unaccounted, it would also appear that mass is being lost and this would also affect the inferred mixing state. However, it is not immediately clear if this effect on mixing would mimic that of a reaction, or precisely how any of these factors will affect the inferred mixing state, and these questions motivate the current work.

In this article we explore the behavior of a gradient based mixing measure, the scalar dissipation rate (see Section 2), under non-conservative conditions. We use non-conservative as a generic term for the effects of changes in mass of individual solutes caused by reactions or mass migrating beyond the monitored extent of the problem space. The fundamental question in this work is, what should the expected behavior of the scalar dissipation rate look like for simple non-conservative systems and can those behaviors be predicted to improve reactive transport models? To this end, we develop a number of analytical relationships that show how mass transformation via reactions affects the inferred mixing state for kinetic reactions with up to three reactants in diffusive systems. Diffusion is considered first in order to address the fundamental behavior of the mixing measure in the presence of reactions and the effects at different Damkohler numbers. The consequences of defining conservative components (e.g. Saaltink et al., 1998) and assuming local equilibrium on the mixing rate are also explored and we show that the mixing state for the component based case cannot be determined from a simple superposition of the individual, solute specific, mixing measures. We then consider the effects of limited monitoring domains on the mixing measures for non-reacting tracers in diffusive and advective–diffusive systems and compare those to the effects of reactions. This work shows that erroneous conclusions about the mixing state can be made if the effects of non-conservative conditions are not accounted for and that reactions can have effects on mixing that are similar to those caused by heterogeneities.

2. Scalar dissipation rates of conservative tracers

The scalar dissipation rate (SDR) is a global mixing measure that is based on the integral of concentration gradients. The SDR has been used in several recent studies of transport in porous media where mixing and reaction rates were investigated (e.g. Bolster et al., 2010, 2011a; Chiogna et al., 2011; Jha et al., 2011) and this recent emergence of the SDR

in hydrogeology further motivates our investigation. The SDR of a passive scalar is defined to be

$$\chi(t) = \int_\Omega D\nabla c(x,t)\cdot\nabla c(x,t)dx \tag{1}$$

where D can be a diffusion or dispersion coefficient that may vary spatially, c is the concentration, $\mathbf{x}$ is a position vector in the domain Ω, t is time, and the integral is taken over the entire domain. The definition of D depends on the type of problem being considered and the use of a diffusion coefficient is only applicable when there is no hydrodynamic dispersion. A similar term lacking the spatial integral can be found in De Simoni et al. (2005), Fernàndez-Garcia et al. (2008) and Luo et al. (2008), among others, and such constructions are common in the mixing and reactive transport literature, often being called a mixing factor. Eq. (1) follows the notation of Le Borgne et al. (2010) but similar definitions can also be found in the physics and engineering literature. The dissipation rate can be determined from the scalar field or the deviations of the scalar field from its mean (e.g. de Dreuzy et al., 2012; Pope, 2000) but in either case Eq. (1) is formally describing the mixing rate using the overall steepness of the concentration gradients; however, this is also a proxy for the mixing state. Consider that a homogeneous scalar field has no variations and the gradients of the concentration field are zero everywhere. When there are variations in solute concentrations, there will be gradients and the SDR will be non-zero. The rate that those gradients are relaxed toward zero is proportionate to the diffusion coefficient and this is quantified by Eq. (1). As mentioned in Section 1, many other mixing measures exist (see also Dentz et al., 2011), but the SDR is a useful tool for describing mixing because it can be approximated without calculating local concentration gradients, and it can be directly related to the global reaction rate in some component based simulations of reactive transport (but only when all of the reactants have the same diffusion coefficient) (Le Borgne et al., 2010). If Eq. (1) is evaluated for a plume experiencing diffusion in an infinite homogeneous domain, translational motion (advection) will not affect the mixing measure. However, translational motion in infinite heterogeneous domains can cause time dependent fluctuation of the mixing state which is the cause of the non-Fickian mixing in Le Borgne et al. (2010). The SDR can be qualitatively understood from Eq. (1), but the SDR can also be approximated from the integral of the squared concentrations:

$$M^2(t) = \int_\Omega c(x,t)^2 dx \tag{2}$$

and the SDR is then given as

$$\chi(t) = -\frac{1}{2}\frac{d}{dt}M^2(t) \tag{3}$$

A similar equation can be found in Kitanidis (1994) for the dilution index, but the expression in that work carries a dependency on the inverse of concentration and is not the same as Eq. (3). It may not be intuitive why Eq. (3) is capable of approximating Eq. (1), but consider that the time rate of change of the integral of the squared concentration will be non-zero unless the solute is perfectly mixed throughout the entire domain. This approximation is exact in a domain with a divergence free velocity field and infinite limits because there is no mass flux outside of the domain. Le Borgne et al. (2010) showed that Eq. (3) was more accurate than the integral in Eq. (1) for homogeneous porous media and Eq. (3) is also computationally more efficient, providing further motivation for using Eq. (3) instead of Eq. (1). We note that Bolster et al. (2010) considered mixing in a plume undergoing space-fractional dispersion and used Eq. (3) as the definition to compute the SDR, most likely because of the presence of a fractional derivative in the dispersion operator. This convention does not maintain the equivalence of Eqs. (1) and (3) since the dispersion operator is non-Fickian, but it is still a valid approach for quantifying mixing. To our knowledge, the behavior of the SDR in time-fractional systems has not been explored in detail but this may be useful since the time-fractional case would maintain the definition of Eq. (1) and produce an alternative form of Eq. (3) that does not involve space-fractional derivatives.

The differences between the SDR defined by Eq. (1) and the integral definition of Eq. (3) have not been studied in detail for non-conservative scalars. Jha et al. (2011) considered the influence of advection on the SDR for a passive tracer but did not derive solutions that can be calculated without evaluating the local concentration gradients and did not investigate the influence of reactions. Analytical solutions of the SDR have been considered by Bolster et al. (2010) and Le Borgne et al. (2010), but these have been presented in the context of specific transport systems and the behavior of the mixing measure when the solute masses vary over time has not been addressed in detail.

3. Dissipation rates in reactive systems

3.1. First-order decay

Many environmental tracers experience first-order, kinetic decay. A common example of this is radioactive decay but many other reaction mechanisms, including biologic processes, can also create first-order decay. Regardless of the mechanism causing the decay, the governing equation we consider is the advection–diffusion-reaction equation (ADRE):

$$\frac{\partial c(x,t)}{\partial t} + \nabla\cdot[v(x)c(x,t)] - \nabla\cdot D\nabla c(x,t) = -\lambda c(x,t) \tag{4}$$

where we will define D as a diffusion coefficient and λ is the decay rate. This equation is most accurate for describing pore-scale reactive transport where the velocity field is fully resolved and thus there is no need for a mechanical dispersion term, but the results may also be applicable to larger support volumes if diffusion/dispersion in the porous medium is strictly stationary. Throughout this section we will assume that the concentration field is known at all locations and times and that the limits of the domain are infinite, but these restrictions will be addressed or relaxed in Section 4. All of these assumptions are made to simplify the solution of these equations and to facilitate the derivation of analytical solutions. Following the derivation of Le Borgne et al. (2010), Appendix A, we can determine the relationship between Eqs. (1) and (3) for first-order decay instead of a passive

solute. Multiply Eq. (4) by $c(x,t)$ and integrate over the entire domain to find:

$$\frac{1}{2}\frac{\partial}{\partial t}\int_\Omega c(x,t)^2 d\Omega + \frac{1}{2}\int_\Omega \nabla\cdot\left[v(x)c(x,t)^2\right]d\Omega - \frac{1}{2}D\int_\Omega \nabla\cdot\nabla c(x,t)^2 d\Omega + \int_\Omega D\nabla c(x,t)\cdot\nabla c(x,t)d\Omega = -\lambda\int_\Omega c(x,t)^2 d\Omega \quad (5)$$

If the problem space is infinite, there will be no net flux out of the domain and the terms involving a divergence operator are zero via the divergence theorem (assuming a divergence free flow field). Eq. (5) then simplifies to:

$$-\frac{1}{2}\frac{\partial}{\partial t}\int_\Omega c(x,t)^2 d\Omega - \lambda\int_\Omega c(x,t)^2 d\Omega = \int_\Omega D\nabla c(x,t)\cdot\nabla c(x,t)d\Omega \quad (6)$$

which recovers the passive case when $\lambda = 0$ and examples of passive and decaying dissipation rates are shown in Fig. 1. We will assume throughout this article that D is constant to further simplify our derivations but note that Eq. (1) does not require this. Eq. (6) corrects the apparent dissipation rate (i.e. Eq. (3)) for mass changes due to decay and permits an unbiased comparison of the behavior of the mixing rates (defined by Eq. (1)) of passive and decaying tracers without needing to evaluate the local gradients. The quantity on the right hand side of Eq. (6) defines what we will refer to as the true or actual dissipation rate which is consistent with Eq. (1) and the definition of the SDR. The expression of Eq. (3) has been used as the tool for quantifying the SDR in the related work (e.g. Bolster et al., 2010; Le Borgne et al., 2010) but, as we already can see in Eq. (6), it will not immediately be equivalent to the actual SDR in non-conservative systems and will require corrections to determine the actual dissipation rates. When the SDR is calculated according to Eq. (3) in a non-conservative system, we will refer to this as the uncorrected dissipation rate. We define the ideal SDR as the analytical solution of Eq. (3) in an infinite domain which is given in Appendix A and appears in Fig. 1 for three values of the diffusion coefficient as the solid, straight lines.

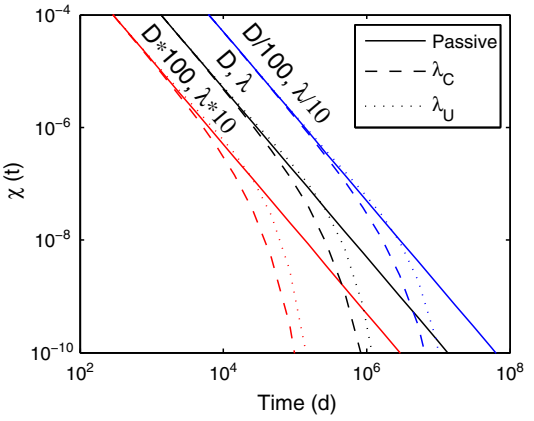

Fig. 1. Analytical solutions for the passive SDR, and the corrected (Eq. (6), λ_C) and uncorrected (Eq. (3), λ_U) SDR for a decaying tracer. Note that the uncorrected SDR slightly overestimates the dissipation rate relative to the infinite domain problem.

The dissipation rate of a decaying tracer can be determined from the dissipation rate of a concentration-normalized passive tracer when the decay constant is known (see Appendix A) from:

$$\chi_\lambda(t) = \chi_0(t)[\exp(-2\lambda t)] \quad (7)$$

where we use subscripts on χ to denote the decay constant; for example $\chi_0(t)$ represents the SDR of a conservative tracer with $\lambda = 0$. Analytical solutions for diffusion with decay in a homogeneous domain using a Gaussian model of diffusion and Eq. (6) are shown in Fig. 1 for several combinations of diffusion and decay constants; in all reactive cases, the SDR predictably approaches zero as the solute mass is consumed. First-order decay is not a complicated reaction and is used here only to illustrate the basic methodology applied throughout Section 3 for the simplest possible reaction. The result of Eq. (7) can also be derived by defining $c(x,t) = c_0(x,t)\exp(-\lambda t)$, where c_0 is a conservative tracer. This change of variables allows Eq. (4) to be used to calculate the SDR without the reaction term; however, in doing so, a conservative component has been defined and we would not be directly considering the behavior of the reactive solute. In this special case, the spatio-temporal evolution of the plume representing the conservative component and the plume of the decaying species are very similar, but we will show in Section 3.2 that this is not necessarily the case for more complex reaction mechanisms.

3.2. Kinetic degradation

Reactions involving multiple species will require additional terms to correct the dissipation rates of the solutes. Consider irreversible decay of solute A to B, both of which are mobile and have the same aqueous phase diffusion coefficient:

$$A \xrightarrow{k} B \quad (8)$$

which evolves forward in time according to the rate laws:

$$\frac{dc_A}{dt} = -kc_A \quad (9a)$$

$$\frac{dc_B}{dt} = kc_A \quad (9b)$$

where the subscripts denote the concentrations of each species and k is the rate constant. Throughout this article we will not explicitly specify the units of the rate constants because they depend on the rate law expression (McQuarrie and Simon, 1997); however, the units of the rate constants can be easily determined from a dimensional analysis of the rate law. We assume unit activity coefficients for simplicity so that activities are analogous to concentrations; this assumes that the concentrations of A and B are dilute (De Simoni et al., 2005; Fernàndez-Garcia et al., 2008). The ADRE of this reactive system will be similar to Eq. (4) where the right hand side of the ADRE is replaced by the right hand side of the rate law expression for each species and we can derive the corrected dissipation rates from the ADREs. The corrected SDR of solute A will be identical to Eq. (6), however solute B will differ:

$$\chi_B(t) = -\frac{1}{2}\frac{\partial}{\partial t}\int_\Omega c_B{}^2 d\Omega + k\int_\Omega c_A c_B d\Omega \quad (10)$$

where we have substituted $c(x,t) \rightarrow c$ for compactness. This is an example of a dissipation rate that depends on the overlap of two species the individual distribution of the solutes since the corrected SDR of the daughter product depends on the concentrations of both species. Intuitively this makes sense because the rate that B is created is controlled by the amount of A that is present, but this will also be affected by the Damkohler number (Da), which is the ratio of the characteristic diffusion and reaction times. Here we define $Da = k/D$ where D is the diffusion coefficient. Notice that the correction in Eq. (10) is additive but the correction in the previous example was not. This reflects the fact that mass is being added to B which increases the dissipation rate by enhancing the spatial gradients of concentration in the area near the source. However, careful inspection of Eqs. (3), (6), and (10) raises an important point that dissipation rates computed from the definition of Eq. (3) may have negative values (e.g. Bolster et al., 2011b) though this is not possible according to Eq. (1). In the absence of electrostatic or other attractive forces, solute mass does not spontaneously agglomerate but instead dissipates and dilutes as the entropy of the system increases towards its maximum (Kitanidis, 1994). Considering this, negative dissipation rates are physically meaningless quantities that arise from not properly accounting for source, sink, or reaction terms.

The behavior of the corrected SDRs for Eq. (9) can be visualized by solving the system of coupled partial differential equations. Since the system is coupled, finding a direct analytical solution can be tedious, so we used the Matlab programming environment to numerically solve the reaction–diffusion system for this example, and the remaining examples that include reactions. The corrected and uncorrected SDRs for both species in Eq. (8) are shown in Fig. 2 and span five orders of magnitude of Da in a 1-D, homogeneous, diffusive domain. Combinations of three values of the rate constant and diffusion coefficient were used to generate the different curves and the differences in diffusion coefficients can be seen by inspecting the point where the SDR intersects the vertical axis. The value of the rate constant determines when the SDR of solute A will approach zero and how long it will take for the SDR of solute B to reach its passive behavior. The diffusion coefficient controls the maximum rate of dissipation but the mixing measure itself is not uniquely affected by Da; different values of D will shift the SDR curves up or down. Overall, the behavior we see in Fig. 2 is a steady increase in the SDR of solute B as it is produced then a transition to passive behavior as solute A is completely consumed. The SDR of solute A predictably falls off exactly like the decay example in the previous section. In contrast, the uncorrected SDR for solute A is an overestimate at all but the earliest times and the uncorrected SDR of solute B is negative until the influence of the reaction ceases. After this point, the uncorrected SDR of B does transition into the expected behavior of a passive tracer, but the negative dissipation rates computed at early times are obviously incorrect.

Sometimes a reactive transport system can be approximated by defining a conservative component (e.g. Cirpka and Valocchi, 2007; De Simoni et al., 2005, 2007; Donado et al., 2009; Sanchez-Vila et al., 2010). This can be done for the system defined by Eq. (8) by adding the two species $c(x,t) = c_A(x,t) + c_B(x,t)$ where c without a subscript denotes the conservative component. Expanding the SDR of the conservative

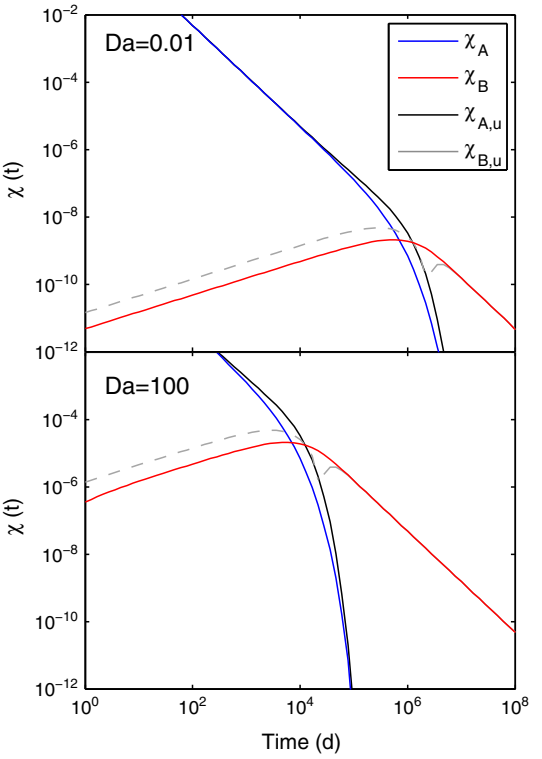

Fig. 2. Corrected and uncorrected scalar dissipation rates for an irreversible bimolecular reaction (Eq. (10)) across five orders of magnitude of Damkohler number (Da). The uncorrected SDRs are denoted with a subscript u in the legend and A and B denote the solutes described in Section 3.2. At late times, the uncorrected SDR for B is identical to the corrected SDR. Dashed lines indicate negative values.

component by inserting its definition into Eq. (3) and simplifying shows:

$$\chi(t) = -\frac{1}{2}\frac{\partial}{\partial t}\int_\Omega {c_A}^2 d\Omega - \frac{\partial}{\partial t}\int_\Omega c_A c_B d\Omega - \frac{1}{2}\frac{\partial}{\partial t}\int_\Omega {c_B}^2 d\Omega \qquad (11)$$

The effects of the reactions on the individual components are nested within the definition of their concentration fields so no reaction terms appear explicitly in Eq. (11) but it is clear that this still depends on the amount of overlap of the solutes and their individual mixing states. The factors driving the SDR of the conservative component can be examined further by incorporating the definition of the corrected SDR. Replacing the left hand side of Eq. (10) with the identity of Eq. (1) and rearranging, the uncorrected dissipation rate can be expressed as

$$-\frac{1}{2}\frac{\partial}{\partial t}\int_\Omega {c_B}^2 d\Omega = \int_\Omega D\nabla c_B \cdot \nabla c_B d\Omega - k\int_\Omega c_A c_B d\Omega \qquad (12)$$

Using this, and a similar expression for solute A, substitution into Eq. (11), shows:

$$\chi(t) = \int_\Omega (D\nabla c_A \cdot \nabla c_A + D\nabla c_B \cdot \nabla c_B) d\Omega + \int_\Omega \left[k c_A (c_A - c_B) - \frac{\partial}{\partial t} c_A c_B \right] d\Omega \qquad (13)$$

The integrals have been grouped to demonstrate that the observed dissipation rate of the conservative component also

involves a time dependent correction. The second term of this dissipation rate can change sign from positive to negative over time but notice that at late times the SDR of A will approach zero and, since this is an irreversible kinetic reaction dependent only on A, we recover the passive dissipation rate of solute B. This example shows that, unlike solutions of the transport equations, the dissipation rate of a multi-component mixture cannot be determined from a simple superposition of the individual dissipation rates and solute interactions must be considered. This result may not be of great concern when the only quantity of interest is the total mass of product formed, or the apparent migration of the conservative component, but this is an important result if one is trying to infer the transport behavior of the individual reactive solutes that make up the component.

To close our analysis of two component systems, consider the effects that a reversible kinetic reaction will have on the dissipation rates:

$$A \underset{k_r}{\overset{k_f}{\Longleftrightarrow}} B \tag{14}$$

where k_f and k_r are the forward and reverse rate constants, respectively. We assume the following rate law for solute A:

$$\frac{dc_A}{dt} = -k_f c_A + k_r c_B \tag{15}$$

We omit the rate law for solute B for brevity since it only differs in the sign of the terms on the right hand side. The corrected SDRs are then:

$$\chi_A(t) = -\frac{1}{2}\frac{\partial}{\partial t}\int_\Omega {c_A}^2 d\Omega - k_f \int_\Omega {c_A}^2 d\Omega + k_r \int_\Omega c_A c_B d\Omega \tag{16a}$$

$$\chi_B(t) = -\frac{1}{2}\frac{\partial}{\partial t}\int_\Omega {c_B}^2 d\Omega + k_f \int_\Omega c_A c_B d\Omega - k_r \int_\Omega {c_B}^2 d\Omega \tag{16b}$$

Again, the dependence of the mixing rate on the overlap of the solutes is immediately apparent even though the reaction rate itself is a linear function of each solute. The behavior of this system for $Da = 0.125$ (using $D = 1 \times 10^{-4}\ m^2/d$, $k_f = 2 \times 10^{-5}$ and $k_r = 5 \times 10^{-6}$) is shown in Fig. 3 which is noticeably different from the behavior seen in Fig. 2. Since the reaction is reversible, it reaches a dynamic equilibrium, but the late time dissipation rates of both solutes differ from the late time behavior predicted by the ideal solution; this is peculiar because both solutes have the same, constant, diffusion coefficient. Solute A transitions into a lower dissipation regime because a significant portion of its mass is converted to B. The reverse reaction rate constant is nearly an order of magnitude less than the forward rate constant so most of the late time mass exists as solute B, hence it's much higher dissipation rate. The general shape of the SDR for solute B is generally the same as it was in Fig. 2, but it never reaches the ideal dissipation rate because the equilibrium state of the reaction at late time causes some mass in the system to always exist as solute A. If an irreversible reaction occurs but the reaction is incomplete (*i.e.* some reactants are not entirely consumed), it will also look like Fig. 3 because the solute masses will have also reached constant values. This is plain to see from Eqs. (9a), (9b) and (10) because if no reaction is occurring the rate constant is effectively zero and the correction to the SDR will also be zero at those times. In Eqs. (16a), (16b) the forward and reverse

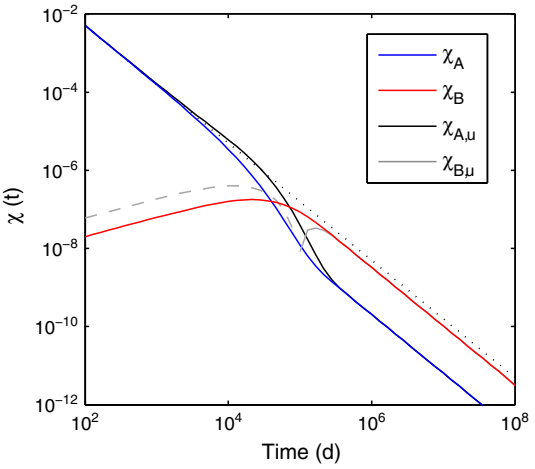

Fig. 3. Scalar dissipation rates for a two component, reversible reaction (Eqs. (16a), (16b)). Dashed lines are negative values and the straight, black dotted line is the ideal SDR. Notice that though both solutes use the same D value, the late time SDRs differ from the ideal model.

reaction corrections balance each other out at equilibrium and scale as $t^{-3/2}$, but the differences in the SDR in this simple, two component system illustrate the importance of understanding how reaction mechanisms can affect mixing rates.

3.3. Multi-component mobile kinetic reaction

The reaction system in the previous example can be further generalized to a mobile, reversible, kinetic reaction with, potentially, unequal forward and reverse rate constants. Consider the three component system:

$$A + B \underset{k_r}{\overset{k_f}{\Longleftrightarrow}} C \tag{17}$$

where A, B and C are solutes, and k_f and k_r represent the rate constants of the forward and reverse reactions, respectively. The rate laws we assume for this reaction are

$$\frac{dcA}{dt} = \frac{dc_B}{dt} = -k_f c_A c_B + k_r c_C \tag{18a}$$

$$\frac{dc_C}{dt} = k_f c_A c_B - k_r c_C \tag{18b}$$

In this case, the corrected dissipation rate for each component will differ from the previous example because of the rate laws and are given by:

$$\chi_A(t) = -\frac{1}{2}\frac{\partial}{\partial t}\int_\Omega {c_A}^2 d\Omega + k_r \int_\Omega c_A c_C d\Omega - k_f \int_\Omega (c_A)^2 c_B d\Omega \tag{19a}$$

$$\chi_B(t) = -\frac{1}{2}\frac{\partial}{\partial t}\int_\Omega {c_B}^2 d\Omega + k_r \int_\Omega c_B c_C d\Omega - k_f \int_\Omega c_A (c_B)^2 d\Omega \tag{19b}$$

$$\chi_C(t) = -\frac{1}{2}\frac{\partial}{\partial t}\int_\Omega {c_C}^2 d\Omega - k_r \int_\Omega {c_C}^2 d\Omega + k_f \int_\Omega c_A c_B c_C d\Omega \tag{19c}$$

These equations correct the individual dissipation rates according to the reactions in a way that is consistent with the reaction mechanism, but, like the previous section, these dissipation rates will deviate from the ideal SDR and the deviations can change over time (Fig. 4). The self-consistency of these equations can be demonstrated by considering a point in the domain where only one solute, say solute A, is present: in the absence of B and C, solute A is passive and the contributions of both corrective terms at that location are zero; thus, the dependence of SDR on the extent to which the solutes overlap is maintained. Three-component kinetic reactions that have non-linear rate laws in one or more components (*e.g.* a rate law proportional to c_A^2) will only differ in the order of the exponents of the last two terms but reactions with more chemical species will have additional variables in the corrective terms. If we define solute C to be a solid precipitate, it is completely immobile (*i.e.* no advection or diffusion) and will not experience mechanical dissipation, however, this will not affect the correction terms of the mobile species since they are determined by the rate law and not the transport equation. Since its concentration will be changing over time, a dissipation rate can be calculated for the immobile component but the general behavior and physical meaning of this rate is different from that of the mobile components.

The SDR for Eq. (17) in a 1-D, homogeneous, diffusive domain is shown in Fig. 4. The initial concentration of A was set to be 3 times greater than B, and C is not present initially. The initial conditions were Dirac delta functions in space at the origin and the forward, and reverse rate constants were arbitrarily set at $k_f = 5 \times 10^{-4}$ and $k_r = k_f/10$. Since the rate constants are uneven, we defined the reaction time scale as the average of the forward and reverse rates which gives $Da = 2.75$ for the example in Fig. 4a, with $D = 1 \times 10^{-4}\ m^2/d$ for all the solutes. Solute A deviated slightly from the ideal SDR because it experiences little change in mass compared to B and C. As we saw in Fig. 2, the uncorrected SDR of the product (solute C) starts negative but the uncorrected SDR of B also becomes negative for a short time. The corrected SDRs all remain positive at all times and the transition into the dynamic equilibrium state can be seen around $t = 10^4 d$. At that time, fluctuations in the SDRs of A and B can be observed and the SDR of C transitions smoothly into its late time regime. This is representative of the mixing state of the system because once the system is in a dynamic equilibrium the concentrations of the solutes appear constant; however, the late time dissipation rate will be controlled by the rate constants and the diffusion coefficient so it will not precisely match an equivalent passive tracer. The effect of solute specific diffusion coefficients is shown in Fig. 4b where $D_A = D$, $D_B = D_A/2$, and $D_C = D_A/10$, but the rate constants are unchanged. The early time behavior of the SDR for solute C was slightly lower than that in Fig. 4a and the transition to the late time behavior occurs faster in Fig. 4b. The magnitude of the fluctuation of the SDR of solute B near $t = 10^4 d$ is slightly enhanced by the reduced diffusion coefficient but the overall behavior is largely unchanged. It is interesting to note that only solute A still scales as $t^{-3/2}$ at late time and the scaling of the other solutes are affected by the rate constants to some extent. For example, solute C scales as $t^{-1/2}$ at early times but scales greater than t^{-2} at late times. This change in the temporal scaling behavior provides evidence that a reaction is strongly influencing the dissipation rate of solute C but it is not a unique indicator of a reaction as we will show in Section 4.

3.4. Connection to equilibrium reactions

The majority of the previous work on mixing in reactive transport systems has assumed that the reactions are not kinetically controlled and are instead equilibrium reactions (Steefel and Lasaga, 1994). This assumption is reasonable when the relaxation time of the reaction is fast relative to the time scale of transport (McQuarrie and Simon, 1997), but this also requires a less often stated assumption of rapid mixing within the support volume Sanchez-Vila et al. (2010). The following precipitation–dissolution reaction has been extensively studied (e.g. De Simoni et al., 2005; Fernàndez-Garcia et al., 2008; Luo et al., 2008):

$$C \Leftrightarrow A + B \tag{20}$$

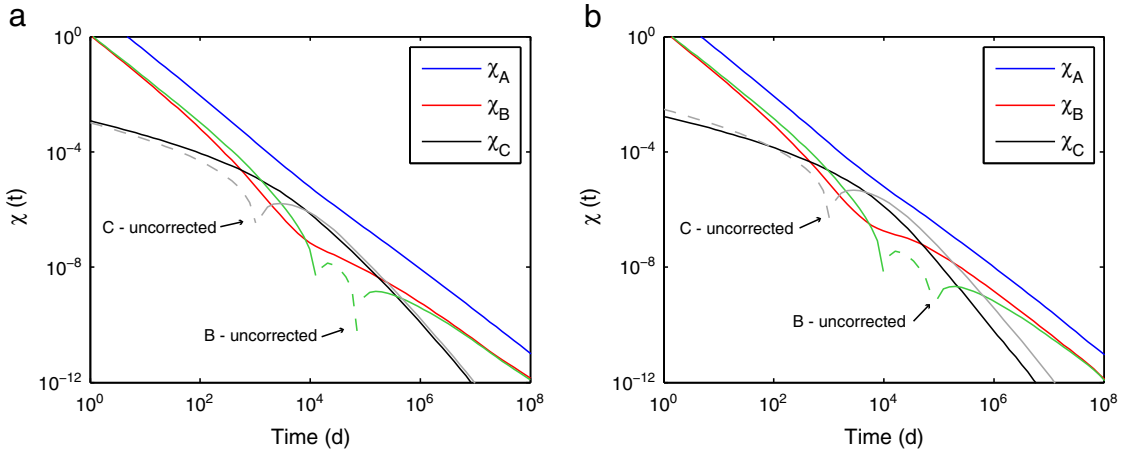

Fig. 4. Scalar dissipation rates for a multi-component kinetic reaction (Eqs. (19a), (19b), (19c)) for a. uniform diffusion coefficients, and b. species specific diffusion coefficients. Dashed lines indicate negative values.

where A and B are mobile solutes and C is an immobile mineral precipitate. This is similar to Section 3.3 except that the direction of the forward and reverse reactions is reversed and no rates are specified because we now assume equilibrium. At all times, a system in dynamic equilibrium must satisfy the local equilibrium expression which, in this case, is

$$k_{eq} = \frac{c_{m,A} c_{m,B}}{c_{im,C}} \tag{21}$$

where k_{eq} is the equilibrium constant for the reaction and we have used the subscripts m and im to denote mobile and immobile phases, respectively. Eq. (21) is typically called the law of mass action (Saaltink et al., 1998) and differs from a rate law because dynamic equilibrium is implied at all times; a rate law specifies the mass transformation rate and implies a finite relaxation time (McQuarrie and Simon, 1997). Given the concentrations of two components and k_{eq}, the concentration of the third component is uniquely defined and any imbalance in the ratio due to physical transport is instantaneously corrected. The condition of chemical equilibrium in any system is achieved when the forward and reverse reaction rates are equal but a state of chemical equilibrium does not imply an equilibrium reaction. Here we take the definition of an equilibrium reaction to imply two key aspects: 1. the system obeys Eq. (21) at all locations with non-zero concentrations, and 2. since the system is in equilibrium relative to the time scale of the model, the rate at which any imbalance to Eq. (21) is corrected is infinitely fast or that the relaxation time is instantaneous. The concentrations (or more precisely the activities) of the products and reactants can vary over space and time and a change in one will cause the system to move to a different equilibrium state but k_{eq} will not change. We specifically list these details to avert any confusion regarding the assumed mechanics of an equilibrium reaction. The previously discussed kinetic reactions can be made to look like equilibrium reactions by using large rate constants; however, a reaction rate is no longer valid because an equilibrium reaction is assumed to be instantaneous [Ginn, 2000].

The scalar dissipation rates of the reaction system defined by Eq. (20) have been studied using a fictitious conservative component that is defined as $c(x,t) = c_{m,A}(x,t) - c_{m,B}(x,t)$. This differs from the conservative component defined in Section 3.2 because the reactions are different. Since $c(x,t)$ is conservative, its dissipation rate can be found from Eq. (3) without any additional corrective terms. Substituting the definition of the conservative component into Eq. (3) gives:

$$\chi(t) = -\frac{1}{2}\frac{\partial}{\partial t}\int_\Omega \left(c_{m,A} - c_{m,B}\right)^2 d\Omega \tag{22}$$

where the lack of subscript on χ will denote the SDR of the conservative component. Expanding the quadratic and distributing the space integral and time derivative gives:

$$\chi(t) = -\frac{1}{2}\frac{\partial}{\partial t}\int_\Omega {c_{m,A}}^2 d\Omega + \frac{\partial}{\partial t}\int_\Omega c_{m,A} c_{m,B} d\Omega - \frac{1}{2}\frac{\partial}{\partial t}\int_\Omega {c_{m,B}}^2 d\Omega \tag{23}$$

The first and third terms on the right hand side are the uncorrected SDRs of solutes A and B and the second term corrects for the reactions. Eq. (23) relates the dissipation rates of the mobile reactive solutes to the fictitious conservative component which is actually an unnormalized mixture. However, if the initial concentrations and sources of A and B are identical, their distributions over space and time will also be identical and the apparent dissipation rate of the conservative component will always be zero even though A and B will still be dissipating. Although these conditions are not likely in most problems of interest, it is important to recognize that the definition of the conservative component can affect the apparent dissipation rate.

Since local equilibrium has been assumed, we can express the concentrations of any of the reacting species using the equilibrium constant expression of Eq. (21). For the precipitation–dissolution of Eq. (20), this can be further simplified by assuming that the activity of the pure mineral C is unity (e.g. Saaltink et al., 1998). Invoking the same assumption, the concentration of B can be expressed using Eq. (23) as $c_{m,B} = k_{eq}(c_{m,A})^{-1}$ and substituting this into Eq. (23) gives

$$\chi(t) = -\frac{1}{2}\frac{\partial}{\partial t}\int_\Omega {c_{m,A}}^2 d\Omega + \frac{\partial}{\partial t}\int_\Omega k_{eq} d\Omega - \frac{{k_{eq}}^2}{2}\frac{\partial}{\partial t}\int_\Omega \left(c_{m,A}\right)^{-2} d\Omega \tag{24}$$

which simplifies to

$$\chi(t) = -\frac{1}{2}\frac{\partial}{\partial t}\int_\Omega {c_{m,A}}^2 d\Omega - {k_{eq}}^2\frac{1}{2}\frac{\partial}{\partial t}\left(c_{m,A}\right)^{-2} d\Omega \tag{25}$$

since the equilibrium constant is invariant with time. In this way, the SDR of the conservative component can be found, given knowledge of the concentration of only solute A and the equilibrium constant, but the correction to Eq. (3) requires the use of a time derivative. This highlights a fundamental difference between dissipation rates that are defined for a conservative component (e.g. Eqs. (11) and (23)), or any other mixture, and those defined for specific solutes: if the reaction is not explicitly accounted for, a time dependent correction to Eq. (3) appears whether the reaction is kinetic or equilibrium. In practice, it is desirable to monitor the concentrations of all the species in the reaction system so we see little advantage to evaluating mixing solely on the basis of the definition of the conservative species besides the mathematical convenience of a conservative tracer; however, considering both the conservative and species dependent dissipation rates may be able to provide insights into the mixing dependency of the reaction history, but to the authors' knowledge this has not yet been investigated.

4. Dissipation rates in restricted domains

One of the limitations to using mixing measures in field studies is the difficulty in evaluating the mixing measure. This often requires complete knowledge of the concentration over time and is impossible to monitor a field scale plume with sufficient resolution to fully resolve the detailed concentration field. The SDR can be applied to numerical and laboratory scale studies that quantify the spatio-temporal concentration field such as Gramling et al. (2002), Zinn et al. (2004), Acharya et al. (2007), Tartakovsky et al. (2008), and Castro-Alcalá et al.

(2012), but upscaling methods to connect the scales are needed. One simple method of doing so is outlined in Section 4.4, but prior to considering that case we develop analytical tools for determining the effects that different limits on the problem domain will have on the dissipation rates.

4.1. Finite symmetric domain

Because a common experimental setup in the laboratory is a column experiment where the average concentration at a plane is monitored, we will use a similar setup as a starting point. For simplicity and comparison to the analytical solutions, we will again assume a homogeneous, 1-D, diffusive domain. If we emplace a solute in the center of a symmetric domain with open boundaries spaced even distances away from the origin and only monitor concentrations within these boundaries (Fig. 5, top), we will see less of the total mass within our domain as time progresses. The observed behavior of the SDR in an infinite domain with a truncated monitoring area that is symmetric about the origin can be found using the following integral:

$$\chi(x,t) = -\frac{1}{2}\frac{\partial}{\partial t}\int_{-x}^{x} c(a,t)^2 da \tag{26}$$

where x is the half-width of the observation window and a is a dummy variable of integration; the lack of subscripts on χ and c denote a passive tracer. The plume will eventually extend beyond the limits in Eq. (26), but we will not allow ourselves knowledge of the concentration field outside of the window from $-x$ to x. We then assume a Gaussian model of concentration with Dirac-delta initial conditions and assume a constant diffusion coefficient (Eq. (A.1), Appendix A). Since the limits of integration are constant and finite, evaluation of the spatial integration and time differentiation is straightforward; however, the solution to Eq. (26) also emerges as limiting case of the general model presented in Appendix B. In either case, the result is:

$$\chi(t|x) = \frac{1}{8\sqrt{2\pi D t^3}}\left[erf\left(x\sqrt{(2Dt)^{-1}}\right) + \frac{\sqrt{2x}}{\sqrt{\pi D t}}\exp\left(\frac{-x^2}{2Dt}\right)\right] \tag{27}$$

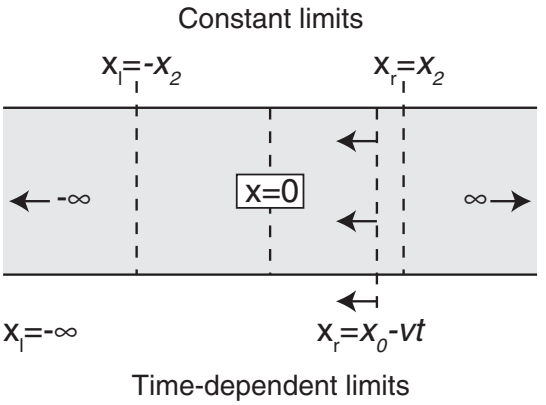

Fig. 5. Illustration of the limited domain integrals for constant (top) and time-dependent (bottom) limits. The problems space (gray area) extends to infinity but we restrict our knowledge to the domain between the dashed lines x_l and x_r.

which is the analytical solution for the SDR for a truncated window of the domain given a constant value of x. The leading factor is the ideal SDR (Appendix A) and the remaining scaling factor causes the SDR to depart from the ideal SDR and transition to scaling behavior other than $t^{-3/2}$ (Fig. 6); recall that similar scaling was also seen in the case of the multi-component kinetic reaction in Section 3.3. The scaling in Eq. (27) shows that the late time concentrations within the domain are still dissipating but that the apparent dissipation rate slows because of mass loss since the most rapidly expanding areas of the plume (the fringes) are no longer included.

Fundamentally, mass loss appears to be the cause for scaling other than $t^{-3/2}$ but the difference is that in Section 3.3 the mass loss was a result of a reaction, whereas in this case it is only an apparent mass loss that results from having an incomplete picture of the domain. The family of curves defined by Eq. (27) also exhibit similar behavior to the non-Fickian mixing shown in Fig. 4b of Le Borgne et al. (2010). The dissipation rates in that work are based on a heterogeneous domain and the departure of the simulated SDR from the infinite domain solution was found to be a function of the variance of the log transformed hydraulic conductivity. Although the size of their domain makes it unlikely that their deviations from the ideal solution are due to domain restrictions, this illustrates the fact that different mechanisms can cause similar kinds of dissipation. The model described by Eq. (27) is relevant to field studies since the areal extent of the aquifer is much larger than a typical high resolution monitoring network. In this case, the problem space is approximately infinite but the domain being monitored is finite.

4.2. Moving boundary

Dissipation in a system experiencing advection and diffusion can also be addressed. One way would be to use the inverse Gaussian model of concentration over time but that distribution carries additional space and time dependencies that are more difficult to manipulate than a diffusion model. However, the squared integral of the concentration in

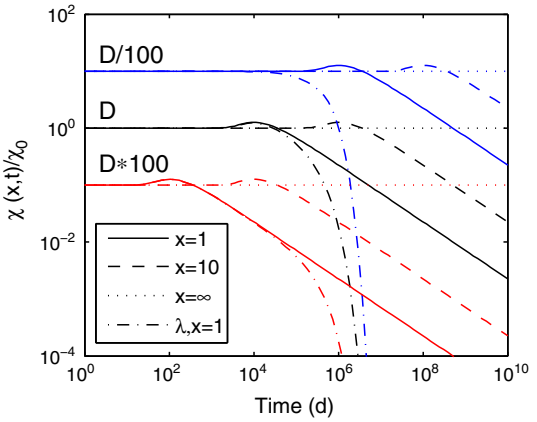

Fig. 6. Behavior of the truncated SDR for three length scales and diffusion coefficients where x is the half-width of the truncated domain. All are normalized to the values based on the ideal solution using $D = 1 \times 10^{-4}\ m^2/d$ and the decay examples all use the same decay constant. These curves are the ratio of Eqs. (29) and (3).

a moving system can be considered in the direction of the 1-D velocity in a similar fashion as the bounded domain by assuming the lower bound to be negative infinity and using a time dependent upper boundary. Conceptually, this is nothing more than Gaussian diffusion with advection in a homogeneous, Lagrangian frame of reference where diffusion in the opposite direction of the velocity is not prohibited. We approximate advection by sliding the upper limit of integration away from its initial position toward negative infinity at a rate defined by the seepage velocity (Fig. 5, bottom). Returning to the definition of the SDR, we now apply a variable upper limit to a passive tracer:

$$\chi(t) = -\frac{1}{2}\frac{\partial}{\partial}\int_{-\infty}^{x(t)} c(a,t)^2 da \tag{28a}$$

$$x(t) = x_0 - vt \tag{28b}$$

where x_0 is the distance of the outlet from the initial condition and v is the constant seepage velocity. The complete derivation is provided in Appendix B (where the time dependent boundary is solved using the Leibniz integral rule) and the solution to Eq. (28) is

$$\chi(t|x_0,v) = \frac{1}{16\sqrt{2\pi Dt^3}}\left\{\begin{array}{l} 1 + erf\left[(x_0 - vt)\sqrt{(2Dt)^{-2}}\right] \\ \quad + \dfrac{\sqrt{2(x_0+vt)}}{\sqrt{\pi Dt}}\exp\left[\dfrac{-(x_0-vt)^2}{2Dt}\right] \end{array}\right\} \tag{29}$$

As x_0 goes to infinity (regardless of the velocity) we recover the infinite domain solution and if the velocity is zero we recover a solution similar to Eq. (27) but the lower bound has been extended to negative infinity. As with the other solutions, decay can be accommodated by scaling the expression for a passive tracer by $\exp(-2\lambda t)$ but notice that this solution cannot account for spatially variable properties in any way.

Eq. (29) provides a basic analytical solution that can be used to describe the mixing state of migrating solutes. The characteristic feature of this model is its sharp peak just before the advection time scale (Fig. 7). The SDR appears to grow because the area of the plume with the highest concentrations, which contributes the largest values to the integral, begins to leave the domain. The extreme asymmetry of the plume within the limits of the integral causes it to look less uniform than it actually is as the center of mass exits, and the plume appears more and more uniform as the low gradient trailing edge passes out of the model. The magnitude of the transition into the sharp peak and the rate at which the solution will approach zero are a function of the Peclet number ($Pe = x_0 v/D$). These effects are shown for three magnitudes of Pe in Fig. 7 for a passive tracer with $D = 1 \times 10^{-4}\ m^2/d$, $x_0 = 5\ m$, and the velocity was calculated to achieve the specified Pe.

Because of its unique behavior, we also provide a comparison of the solution predicted by Eq. (29) and an explicit pore-scale model of transport that was available to the authors. The model uses standard Lattice-Boltzmann methods to simulate transport through a column of medium-coarse sand about 6 cm in length; the model was presented by Engdahl and Fogg (2011). The SDR from that model (curve 7, Fig. 8) exhibits the same characteristics as Eq. (29) but also contains some noise likely caused by the explicitly resolved geometry. We note that the behavior of the solutions to Eq. (29) exhibits similarities to the finite domain solutions of concentration fluctuations shown by Bolster et al. (2012). It is also possible to allow the plume to diffuse for some time before it enters the problem domain. This can be done by shifting both boundaries as outlined in Appendix B. The results of this operation depend heavily on the functions that define the time-dependent limits but doing so can produce early time dissipation rates well below the infinite domain solution (curve 6, Fig. 8) and negative values could be computed.

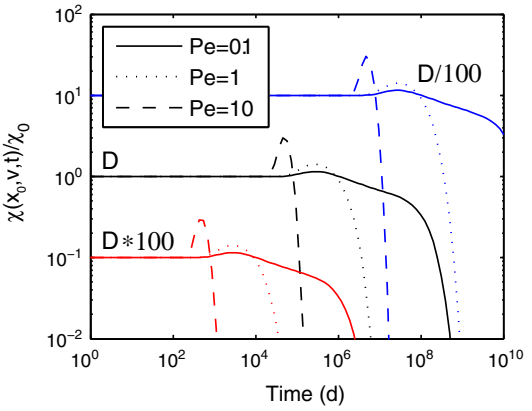

Fig. 7. Moving boundary SDR for three diffusion coefficients and Peclet numbers. All are normalized to the infinite domain solution with $D = 1 \times 10^{-4}\ m^2/d$ and $x_0 = 5\ m$. Note the rapid rise above the infinite domain solution and the rapid drop for $Pe > 1$. These curves are the ratio of Eqs. (31) and (3).

4.3. Fully bounded domain

Next we consider a domain with finite closed limits that do not allow solute fluxes, similar to a batch reactor. The effects of such boundaries are an important consideration

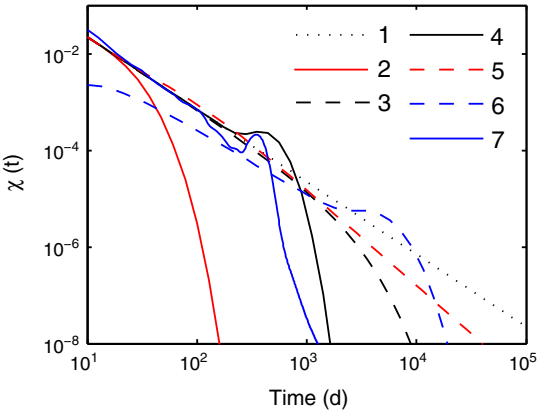

Fig. 8. Comparison of the general shapes of several of the different models presented here with the corresponding equations in parentheses: 1. Ideal solution (A.3); 2. Bounded passive domain (32); 3. Infinite domain with decay (7); 4. One-sided moving boundary (31); 5. Truncated domain (29); 6. Two-sided moving boundary with $Pe = 5$ (B.8); and 7. Explicit pore-scale simulation of advective–diffusive transport (Engdahl and Fogg, 2011).

since solute mass will be forced to accumulate rather than exit the area; this is in contrast to Sections 4.1 and 4.2 where the integral was restricted but the problem space was still infinite. This problem is deceptive because it cannot be solved in the same fashion as the previous examples since the boundary condition fundamentally changes the late time behavior of the plume. One way to approximate this solution is to use Eq. (3) with a model of the concentration field that is a superposition of an infinite number of solutions to Eq. (4) for passive diffusion that are sequentially shifted away from the origin as

$$c(x,t) = \frac{1}{\sqrt{4\pi Dt}} \sum_{n=-\infty}^{\infty} \exp\left(\frac{(x+nL)^2}{4Dt}\right) \tag{30}$$

where n is the integer index, L is the total width of the symmetric, bounded domain, and the initial condition is a Dirac-delta centered at the origin. The SDR based on this model of the concentration can be numerically approximated with a finite series provided that the series is large enough to enforce the zero flux condition at $x = L/2$ which should give a constant concentration at late times. At early times the system will behave the same as the infinite domain problem but as time progresses the concentration within the domain will reach a constant uniform value because there is no effluent. The solid boundary will increase the concentration at the limits of the domain and increase the squared mass at the edge relative to the same location in an equivalent open boundary system. This will cause the dissipation rate to approach zero much more rapidly than in the open boundary case once a significant portion of the mass reaches the edges of the domain. The dissipation rate will continue to decrease and asymptotically approach zero at late times, but for all effective purposes the domain becomes a homogeneous uniform mixture.

The amount of time it should take for deviations from the infinite domain to become visible will depend on the characteristic diffusion time scale, $(L/2)^2/D$ in this case, but mass will being to accumulate before this time, thus, we should expect deviations to occur below the characteristic diffusion time. In Fig. 8 we include a highly discretized numerical approximation of the SDR computed by Eq. (3) with the concentration defined by Eq. (30). The domain has width $L = 2\ m$, $D = 1 \times 10^{-4}\ m^2/d$, and $n = 400$ was sufficient to enforce the zero flux boundary at $x = 1\ m$ over the simulated time scale. The model exhibits the expected behaviors, and the SDR rapidly goes to zero near the diffusion time scale. However, notice that it tends to zero more slowly than in the case of the moving boundary dissipation rate, but that the deviations of the finite, bounded, domain are much greater at early times than the moving boundary. Some of these differences shown in Fig. 8 are due to the sensitivity of the moving boundary solution to the Peclet number. To address this we varied *Pe* of the moving boundary solutions across 5 orders of magnitude. The advection signature dominates for $Pe > 1$; this regime is characterized by a higher than ideal dissipation rate as we approach the advective time scale and a rapid drop toward zero afterward that is proportional to *Pe*. For $Pe < 1$, the advection signature steadily diminishes but the transition from higher than ideal dissipation towards lower than ideal dissipation occurs at the characteristic diffusion time. In contrast, the bounded domain solution calculated from Eq. (30) never exceeds the ideal, infinite domain SDR and reaches zero by $(L/2)^2/D$. Thus, regardless of particular choices of v and D, the defining characteristic that separates these two solutions is whether the SDR reaches, or passes, zero before or after the diffusion time scale.

4.4. Inferring dissipation rates from effluent concentrations

The previous derivations have all assumed complete knowledge of the concentration field at all times. Such knowledge is unlikely in field settings and also in many laboratory experimental setups. A more common source of concentration is the effluent breakthrough curve (BTC) of a passive tracer. BTCs cannot be used to directly quantify the dissipation rate because a BTC does not uniquely represent the spatial variability of the concentration field within the domain and usually includes the combined effects of diffusion and dispersion. Certainly BTCs and the SDR are related but a generalized analytical connection has not been developed and is not necessary in some cases. The simplest way to infer the SDR from the BTC of a passive diffusing tracer is to assume a model for the concentration field and determine the diffusion coefficient by fitting the BTC. The analytical solution for the passive SDR in a homogeneous, 1-D, diffusive domain is given in Appendix A (Eq. (A.3)) and only requires the distance from the source and the diffusion coefficient from a BTC. This is only possible because there is no spatial variability in the aquifer and diffusion is symmetric (or isotropic if generalized to more spatial dimensions) so mixing and spreading are analogous in this special case. In heterogeneous systems it will certainly be necessary to delineate the effects of dispersion to correctly infer the mixing state. If the tracer is undergoing first order decay, the decay constant must also be determined, but this can also be accomplished by fitting the effluent BTC or by use of an objective function approach such as Eqs. (9a), (9b). It is also possible to assume a model other than the Gaussian distribution for the concentration field (e.g. Bolster et al., 2010). Doing so requires computation of the appropriate analytical solution of the SDR. There are a number of physically plausible distributions, such as the Levy distribution, that will be difficult to integrate analytically, but numerical approximations may be possible.

Instead of assuming a single distribution, the behavior of the tracer can also be approximated using a linear combination of tracers. For simplicity we will only describe the case where our 1-D plume is described by a weighting of two tracers having different diffusion coefficients. The SDR in an infinite domain can then be determined by solving the following expression

$$\chi_{c_1+c_2}(t) = -\frac{1}{2}\frac{\partial}{\partial t}\int \left[\alpha c_1\left(x,t|D_1\right) + \beta c_2(x,t|D_2)\right]^2 dx \tag{31}$$

where the subscripts 1 and 2 delineate the concentrations and diffusion coefficients of the two plumes, and α and β are the relative fractional contributions of each plume that must sum to unity. The analytical solution to this equation is lengthy and involves multiple correction terms (which can be further generalized, and greatly complicated, by permitting decay at different rates and different initial locations), but it can be found using the procedures in Appendix B.

However, it is sufficient to recognize that this equation is nothing more than a normalized equivalent of Eq. (22) and, as such, the dissipation rate of the mixture will not be a superposition of the individual dissipation rates, even if both are passive. Unlike Eq. (22), if both solutes initially have unit concentrations, the total mixture will also have unit concentration. We note that the solution of Eq. (31) is conceptually similar to the analytical solution derived by Bolster et al. (2011a), who described mixing in a two dimensional system using two values of the diffusion coefficient. Bolster et al. (2011a) is one of the few studies that evaluated mixing measures where different diffusion coefficients were used for different solutes and more investigations like this are needed.

5. Discussion

The behavior of the scalar dissipation rate, if calculated from Eq. (3), can be strongly influenced by the reactions and domain limitations that we have considered here (Fig. 8). Most significant is the similarity of our truncated domain analytical solution (Eq. (27) and curve 5 in Fig. 8) and the non-Fickian mixing shown by Le Borgne et al. (2010). Both solutions depart from the infinite domain solution and transition to similar, stable, dissipation regimes, yet Le Borgne et al. used $Pe = 100$ and Eq. (27) has $Pe = 0$. Part of the discrepancy may lie in the definition of Pe which we defined as the distance from the source to the limit of our window of integration whereas Le Borgne et al. define Pe in terms of a characteristic heterogeneity length scale that is much smaller than the domain size. If we use a smaller characteristic length scale, our Pe would significantly decrease in the moving boundary problem, however, redefining the length scale will not affect Pe in Eq. (27) since $v = 0$. A generalized form of the moving boundary solution where the upper and lower bounds are time dependent (Appendix B, Eqs. (B.6a), (B.6b)) can reproduce the non-Fickian mixing signature up to a point but eventually goes to zero as the plume exits the domain if the velocity remains finite at late times. The bounds on the model of Le Borgne et al. were reported to be large relative to the problem size and we expect that a signature like that described by Eq. (29) would have been observed if significant mass loss had occurred. Even though the deviations from the ideal solution stem from two fundamentally different causes, they have similar effects on the inferred mixing state. This highlights the important point that erroneous conclusions about mixing can be made if domain limitations, reactions, and heterogeneity effects are not considered.

The main advantage of the methods we have outlined here is that none of them require evaluation of the local concentration gradients. If a homogeneous continuum is used in an Eulerian simulation, it is possible to use a spatial discretization of the domain that is fine enough to resolve the local concentration gradients so that Eq. (1) will be reasonably accurate. Although we do not include it here, this was done to verify the corrections derived in Section 3. However, if using a finite number of particles, or models with complex geometries where the concentration field can vary greatly over short distances, the local gradient approximation of the SDR can easily fail (Le Borgne et al., 2010). Another important point is that the SDR represented in Section 4 may not be precisely equivalent to one that explicitly accounts for solute fluxes (e.g. Eq. (5)) but it does represent the view of the SDR that one would observe for the given conditions and avoids potential errors from computing the local gradients. In most of the examples of Section 4, the scaling factor that relates the observed dissipation rates to the analytical solution in an infinite domain can be used to convert problems having different boundary conditions, domain limits, or reaction systems into a standardized frame of reference for dissipation and reactions. For example, the SDR of a passive tracer in a finite, advection-free, domain can be converted into an equivalent dissipation rate for a decaying tracer in a mobile system composed of the same material. This is possible because the limited domain scaling terms were all expressed relative to the SDR in an infinite passive domain which serves as a common factor that connects all of the solutions. The main limitation of this is that all of the corrections require knowledge of the diffusion coefficient(s) and most required a single D value for all solutes. It may be possible to circumvent the former by expressing the deviation of the observed SDR from an equivalent macro-dispersive model, similar to de Dreuzy et al. (2012) but this has not been done yet.

Although we have exclusively focused on the scalar dissipation rate, it should be clear that limited domains and reactions can affect other mixing measures as well. Since the SDR is formally defined for a passive tracer, it could be argued that the corrections we developed in Section 3 are measuring something entirely different. However, consider that first-order, dual-domain mass transfer can be modeled in exactly the same way as the reversible kinetic reaction of Eq. (14) (though we note that the similarity of the mass-transfer case to Fig. 3 will depend on whether diffusion is permitted in the immobile domain and the magnitude of the immobile D if it is non-zero). Mass transfer was not considered in this work due to length constraints, but it is straight forward to recognize conceptually that the conversion of mass from one "phase" to another, whether via a chemical reaction or immobile mass transfer, affects the inferred mixing state. Regardless of whether the definition of the SDR is precisely maintained, the reaction corrections to Eq. (3) provide an alternative to Eq. (1) for describing the mixing state of reactive solutes, similar to the work of Bolster et al. (2010) who also deviated from the strict definition of Eq. (1).

In summary, a number of corrections were derived that allow scalar dissipation rates in non-conservative systems to be evaluated without computing local concentration gradients, and this also highlighted how reaction mechanisms can effect dissipation rates. We began with a number of examples based on reaction systems of increasing complexity in infinite domains. For a tracer undergoing first order decay, the SDR of the decaying tracer is the SDR of an equivalent passive tracer scaled by $\exp(-2\lambda t)$. Multi-component kinetic and equilibrium reactions require similar corrections that depend on the rate laws or mass action laws governing the chemical reactions. Corrections were then derived to account for the effects of finite domain limits on the dissipation rate, and these factors affect the SDR regardless of how it is computed. The SDR evaluated in a truncated domain exhibited trends that are similar to non-Fickian mixing, highlighting the importance of considering domain limitation and boundary effects on mixing measures; but some of the limited domain behavior also resembled the dissipation rates of a multi-component kinetic reaction in an infinite domain. The similarity to non-Fickian

mixing also implies that it may be possible to derive corrections, similar to those we derived here, that account for the influence of heterogeneities on the dissipation rates.

Acknowledgments

The authors thank the anonymous reviewers for their constructive comments that significantly improved the quality of this manuscript. The project described was supported by award number P42ES004699 from the National Institute of Environmental Health Sciences. The content is solely the responsibility of the author and does not necessarily represent the official views of the National Institute of Environmental Health Sciences or the National Institute of Health.

Appendix A. Scalar dissipation rate of a decaying solute

Here we derive the analytical solution for the corrected scalar dissipation rate (SDR) of a decaying solute. Assume that a unit concentration tracer is released instantaneously in the center of an infinite 1-D, homogeneous domain with zero velocity. In the tracer is conservative, the spatial distribution of concentrations will follow Fick's law of diffusion at all times, the solution of which is the Gaussian distribution:

$$c_0(x,t) = \frac{1}{\sqrt{4\pi Dt}} \exp\left(-\frac{x^2}{4Dt}\right) \tag{A.1}$$

where D quantifies the strength of the diffusion process and subscripts will denote the decay rate throughout this appendix. The decay rate is zero in Eq. (A.1) since the tracer is passive. Also note that we assume a normalized initial concentration for simplicity. Integrating the square of Eq. (A.1) over all space gives

$$\int_{-\infty}^{\infty} c_0(x,t)^2 \mathrm{d}x = \frac{1}{\sqrt{8\pi Dt}} = M_0^2(t) \tag{A.2}$$

Since the domain is infinite, there will be no solute flux out of the domain at any time and the analytical solution for the SDR over time can then be found (see Eq. (5)) which is

$$\chi_0(t) = -\frac{1}{2}\frac{\partial}{\partial t} M_0^2(t) = \frac{1}{8\sqrt{2\pi Dt^3}} \tag{A.3}$$

This solution is identical to Eqs. (9a), (9b) of Le Borgne et al. (2010) when a unit concentration and unit width of a 2-D domain are used in their equation. This can also be derived by inserting Eq. (A.1) into Eq. (1) and solving for an infinite domain. If the tracer decays according to a first order rate law, the distribution of the solute from Eq. (A.1) becomes

$$c_\lambda(x,t) = \frac{\exp(-\lambda t)}{\sqrt{4\pi Dt}} \exp\left(-\frac{x^2}{4Dt}\right) \tag{A.4}$$

where λ is the decay constant. Integrate the square of Eq. (A.4) over all space to find

$$\int_{-\infty}^{\infty} c_\lambda(x,t)^2 \mathrm{d}x = 2\left[\frac{\exp(-2\lambda t)}{\sqrt{32\pi Dt}}\right] = 2M_\lambda^2(t) \tag{A.5}$$

Applying the product rule, the time derivative of Eq. (A.5) is

$$-\frac{1}{2}\frac{\partial}{\partial t} M_\lambda^2(t) = M_\lambda^2(t)\left[2\lambda + \frac{1}{4t}\right] \tag{A.6}$$

where have also introduced the −½ scaling necessary to calculate the SDR. According to Eq. (6), the corrected SDR for a decaying tracer is found from

$$\begin{aligned}\chi_\lambda(t) &= -\frac{1}{2}\frac{\partial}{\partial t} M_\lambda^2(t) - \lambda M_\lambda^2(t) \\ &= M_\lambda^2(t)\left[2\lambda + \frac{1}{4t}\right] - 2\lambda M_\lambda^2(t)\end{aligned} \tag{A.7}$$

inserting the appropriate definitions gives

$$\chi_\lambda(t) = \frac{M_\lambda^2(t)}{4t} = \frac{\exp(-2\lambda t)}{4t\sqrt{32\pi Dt}} \tag{A.8}$$

The terms of the denominator are the SDR of a passive tracer from Eq. (A.5), so we can rewrite Eq. (A.8) as

$$\chi_\lambda(t) = \frac{\exp(-2\lambda t)}{8\sqrt{2\pi Dt^3}} = \chi_0(t)\exp(-2\lambda t) \tag{A.9}$$

which is the corrected dissipation rate of a decaying tracer over time expressed in terms of the dissipation rate of a passive tracer and a decay constant. This relationship holds for all of the models presented here in that the solution for a passive tracer in any configuration need only be scaled by the square of the decay term. For example, combining the decay elements of this section with the tools of Appendix B shows that the limited domain integral about the origin that defines the SDR of a decaying tracer is

$$\chi_\lambda(t|x) = \frac{\exp(-2\lambda t)}{8\sqrt{2\pi Dt^3}}\left[\mathrm{erf}\left(x\sqrt{(2Dt)^{-1}}\right) + \frac{\sqrt{2}x}{\sqrt{\pi Dt}}\exp\left(\frac{-x^2}{2Dt}\right)\right] \tag{A.10}$$

which is Eq. (29) scaled by the correction for first order decay. The relationship of the passive and decaying tracers in Eq. (A.9) can also be found by changing variables in Eq. (4) such that $c = c'\exp(-\lambda t)$ where c' is a dummy variable. The differential Equation is then solved in terms of c' and the definition of c is substituted back into the solution to recover Eq. (A.9). This is a special case where defining a conservative component recovers the actual dissipation rates because only one species is being considered.

Appendix B. Scalar dissipation rates in finite domains

The analytical solutions in Section 4 all deal with scalar dissipation rates in an infinite domain where only a subset of the problem space is considered. Except for the specific case of impermeable walls where there is no effluent (Section 4.3), the other analytical solutions are limiting cases of the following integral:

$$\chi_0(t) = -\frac{1}{2}\frac{\partial}{\partial t}\int_{a(t)}^{b(t)} c(x,t)^2 \mathrm{d}x \tag{B.1}$$

where the limits of the integral are allowed to be arbitrary time dependent functions and the subscript zero denotes a passive tracer. Time differentiation of an integral with time dependent limits can be solved using the Leibniz integral rule which is

$$\frac{\partial}{\partial t}\int_{a(t)}^{b(t)} f(x,t)\mathrm{d}x = \int_{a(t)}^{b(t)} \frac{\partial f}{\partial t}\mathrm{d}x + f(b(t),t)\frac{\partial b}{\partial t} - f(a(t),t)\frac{\partial a}{\partial t} \tag{B.2}$$

where a and b are, again, arbitrary time dependent functions and f is function in x and t. Adopting the Gaussian diffusion model without decay:

$$f = c(x,t)^2 = \frac{1}{4\pi Dt}\exp\left(-\frac{x^2}{2Dt}\right) \tag{B.3}$$

where D is the diffusion coefficient. The time derivative of this function is:

$$\frac{\partial f}{\partial t} = \exp\left(-\frac{x^2}{2Dt}\right)\left[\frac{x^2}{8\pi D^2 t^3} - \frac{1}{4\pi Dt^2}\right] \tag{B.4}$$

which is then integrated to give:

$$\int_{a(t)}^{b(t)} \frac{\partial f}{\partial t}\mathrm{d}x = \frac{-1}{8\sqrt{2\pi Dt^3}}\left[\mathrm{erf}\left(x\sqrt{\frac{1}{2Dt}}\right) + \frac{\sqrt{2}x}{\sqrt{\pi Dt}}\exp\left(-\frac{x^2}{2Dt}\right)\right]\Bigg|_{b(t)}^{a(t)} \tag{B.5}$$

where erf is the error function. The general solution for any set of boundaries is found by inserting this and the other requisite terms into Eq. (B.2), which is then scaled by −½ to determine the apparent SDR for that particular problem. With some algebra, it can be shown that the general solution of Eq. (B.1) is:

$$\chi_0(t|a,b) = \frac{1}{16\sqrt{2\pi Dt^3}}[\psi(t|b) - \psi(t|a)] \tag{B.6a}$$

with

$$\psi(t|y) = \mathrm{erf}\left(y\sqrt{\frac{1}{2Dt}}\right) + \frac{\sqrt{2}}{\sqrt{\pi Dt}}\left(y - 2t\frac{\partial y}{\partial t}\right)\exp\left(\frac{-y^2}{2Dt}\right) \tag{B.6b}$$

where y is an arbitrary, differentiable, function. Notice that only one term requires the time derivative of y and the remaining terms are evaluated using the function. Toward an expression for a system experiencing diffusion and advection, we now define time dependent functions to dictate the limits:

$$b(t) = x_2 - vt \tag{B.7a}$$

$$a(t) = x_1 - vt \tag{B.7b}$$

where x_1 and x_2 are the initial positions of the lower and upper boundaries, respectively, and the velocity of each boundary is assumed constant and identical at velocity v; the latter assumption is not required but is invoked for simplicity. The time derivative of both functions is $-v$ and inserting the appropriate functions into Eq. (B.6) gives

$$\chi_0(t|x_1,x_2,v) = \frac{1}{16\sqrt{2\pi Dt^3}}[\psi_2(t|x_2,v) - \psi_1(t|x_1,v)] \tag{B.8a}$$

with

$$\psi_i(t|x_i,v) = \mathrm{erf}\left[(x_i - vt)\sqrt{\frac{1}{2Dt}}\right] + \frac{\sqrt{2}(x_i+vt)}{\sqrt{\pi Dt}}\exp\left[\frac{-(x_i-vt)^2}{2Dt}\right] \tag{B.8b}$$

This allows any arbitrary portion of the plume to be integrated and can be used to approximate advective–diffusive transport in a homogeneous domain. Allow $x_2 \to \infty$ and $x_1 \to -\infty$; both exponential terms will go to zero, $\mathrm{erf}(\infty) - \mathrm{erf}(-\infty) = 2$, and the analytical solution in an infinite domain is recovered. If only x_1 goes to negative infinity and the upper limit of integration is governed by Eq. (B.7a), the exponential in x_1 goes to zero and the error function term in x_1 is −1 resulting in:

$$\chi_0(t|-\infty,x_2,v) = \frac{1}{16\sqrt{2\pi Dt^3}}[1 + \psi_2(t|x_2,v)] \tag{B.9}$$

This solution is most similar to an advection–diffusion model in a finite domain where the center of mass exits the model domain at time L/v, where L is the 1-D length from the source to the monitoring location. Finally, if we allow a velocity of zero and require symmetric, constant limits on our integral, we see that $\psi_1 = -\psi_2$; $(\psi_2 - \psi_1) = 2\psi_2$ and simplification shows:

$$\chi_0(t|x) = \frac{1}{8\sqrt{2\pi Dt^3}}[\psi_2(t|x,v=0)] \tag{B.10}$$

which is our Eq. (29) using the definition of Eq. (B.8b). The same procedure can be used for decaying tracers and the result will obey the expression of Eq. (7) regardless of the particular limits imposed on the integral.

References

Acharya, R.C., Valocchi, A.J., Werth, C.J., Willingham, T.W., 2007. Pore-scale simulation of dispersion and reaction along a transverse mixing zone in two-dimensional porous media. Water Resources Research 43 (10), 1–11. http://dx.doi.org/10.1029/2007WR005969.

Battiato, I., Tartakovsky, D.M., Tartakovsky, A.M., Scheibe, T., 2009. On breakdown of macroscopic models of mixing-controlled heterogeneous reactions in porous media. Advances in Water Resources 32 (11), 1664–1673. http://dx.doi.org/10.1016/j.advwatres.2009.08.008.

Bolster, D., Benson, D., Le Borgne, T., Dentz, M., 2010. Anomalous mixing and reaction induced by superdiffusive nonlocal transport. Physical Review E 82 (2), 1–5. http://dx.doi.org/10.1103/PhysRevE.82.021119.

Bolster, D., Dentz, M., Le Borgne, T., 2011a. Hypermixing in linear shear flow. Water Resources Research 47 (9), 1–5. http://dx.doi.org/10.1029/2011WR010737.

Bolster, D., Valdés-Parada, F.J., LeBorgne, T., Dentz, M., Carrera, J., 2011b. Mixing in confined stratified aquifers. Journal of Contaminant Hydrology 120–121, 198–212. http://dx.doi.org/10.1016/j.jconhyd.2010.02.003.

Bolster, D., de Anna, P., Benson, D.A., Tartakovsky, A.M., 2012. Incomplete mixing and reactions with fractional dispersion. Advances in Water Resources 37, 86–93. http://dx.doi.org/10.1016/j.advwatres.2011.11.005.

Castro-Alcalá, E., Fernàndez-Garcia, D., Carrera, J., Bolster, D., 2012. Visualization of mixing processes in a heterogeneous sand box aquifer. Environmental

Science & Technology 46 (6), 3228–3235. http://dx.doi.org/10.1021/es201779p.
Chiogna, G., Cirpka, O.A., Grathwohl, P., Rolle, M., 2011. Relevance of local compound-specific transverse dispersion for conservative and reactive mixing in heterogeneous porous media. Water Resources Research 47 (7). http://dx.doi.org/10.1029/2010WR010270.
Chiogna, G., Hochstetler, D.L., Bellin, A., Kitanidis, P.K., Rolle, M., 2012. Mixing, entropy, and reactive solute transport. Geophysical Research Letters 39, L20405. http://dx.doi.org/10.1029/2012GL053295.
Cirpka, O.A., Kitanidis, P.K., 2000. Characterization of mixing and dilution in heterogeneous aquifers by means of local temporal moments. Water Resources Research 36 (5), 1221–1236.
Cirpka, O.A., Valocchi, A.J., 2007. Two-dimensional concentration distribution for mixing-controlled bioreactive transport in steady state. Advances in Water Resources 30 (6–7), 1668–1679. http://dx.doi.org/10.1016/j.advwatres.2006.05.022.
de Dreuzy, J.-R., Carrera, J., Dentz, M., Le Borgne, T., 2012. Time evolution of mixing in heterogeneous porous media. Water Resources Research 48 (6). http://dx.doi.org/10.1029/2011WR011360 in press.
De Simoni, M., Carrera, J., Sánchez-Vila, X., Guadagnini, A., 2005. A procedure for the solution of multicomponent reactive transport problems. Water Resources Research 41 (11), 1–16. http://dx.doi.org/10.1029/2005WR004056.
De Simoni, M., Sanchez-Vila, X., Carrera, J., Saaltink, M.W., 2007. A mixing ratios-based formulation for multicomponent reactive transport. Water Resources Research 43 (7), 1–10. http://dx.doi.org/10.1029/2006WR005256.
Dentz, M., Le Borgne, T., Englert, A., Bijeljic, B., 2011. Mixing, spreading and reaction in heterogeneous media: a brief review. Journal of Contaminant Hydrology 120–121, 1–17. http://dx.doi.org/10.1016/j.jconhyd.2010.05.002.
Donado, L.D., Sanchez-Vila, X., Dentz, M., Carrera, J., Bolster, D., 2009. Multicomponent reactive transport in multicontinuum media. Water Resources Research 45 (11), 1–11. http://dx.doi.org/10.1029/2008WR006823.
Engdahl, N.B., Fogg, G.E., 2011. Direct upscaling of kinetically controlled reactive transport with mobile–immobile mass transfer. Abstract H31E-1209 presented at 2011 Fall Meeting AGU, San Francisco, Calif., 5–9 Dec.
Fernàndez-Garcia, D., Sánchez-Vila, X., Guadagnini, A., 2008. Reaction rates and effective parameters in stratified aquifers. Advances in Water Resources 31 (10), 1364–1376. http://dx.doi.org/10.1016/j.advwatres.2008.07.001.
Ginn, T.R., 2000. On the distribution of multicomponent mixtures over generalized exposure time in subsurface flow and reactive transport: theory and formulations for residence-time-dependent sorption/desorption with memory. Water Resources Research 36 (10), 2885–2893.
Gramling, C.M., Harvey, C.F., Meigs, L.C., 2002. Reactive transport in porous media: a comparison of model prediction with laboratory visualization. Environmental Science & Technology 36 (11), 2508–2514.
Jha, B., Cueto-Felgueroso, L., Juanes, R., 2011. Quantifying mixing in viscously unstable porous media flows. Physical Review E 84 (6). http://dx.doi.org/10.1103/PhysRevE.84.066312.
Kapoor, V., Gelhar, L.W., 1994. Transport in three-dimensionally heterogeneous aquifers 1. Dynamics of concentration fluctuations. Water Resources Research 30 (6), 1775–1788.
Kapoor, V., Gelhar, L.W., Miralles-Wilhelm, F., 1997. Bimolecular second-order reactions in spatially varying flows: segregation induced scale-dependent transformation rates. Water Resources Research 33 (4), 527–536.
Kitanidis, P.K., 1994. The concept of the dilution index. Water Resources Research 30 (7), 2011–2026.
Le Borgne, T., Dentz, M., Bolster, D., Carrera, J., de Dreuzy, J.-R., Davy, P., 2010. Non-Fickian mixing: temporal evolution of the scalar dissipation rate in heterogeneous porous media. Advances in Water Resources 33 (12), 1468–1475. http://dx.doi.org/10.1016/j.advwatres.2010.08.006.
Le Borgne, T., Dentz, M., Davy, P., Bolster, D., Carrera, J., de Dreuzy, J.-R., Bour, O., 2011. Persistence of incomplete mixing: a key to anomalous transport. Physical Review E 84 (1), 1–4. http://dx.doi.org/10.1103/PhysRevE.84.015301.
Luo, J., Dentz, M., Carrera, J., Kitanidis, P., 2008. Effective reaction parameters for mixing controlled reactions in heterogeneous media. Water Resources Research 44 (2), 1–12. http://dx.doi.org/10.1029/2006WR005658.
McQuarrie, D.A., Simon, J.D., 1997. Physical Chemistry: A molecular Approach. University Science Books, Sausalito, CA.
Miralles-Wilhelm, F., Gelhar, L.W., Kapoor, V., 1997. Stochastic analysis of oxygen-limited biodegradation in three-dimensionally heterogeneous aquifers. Water Resources Research 33 (6), 1251–1263.
Pope, S.B., 2000. Turbulent Flows. Cambridge University Press.
Raje, D.S., Kapoor, V., 2000. Experimental study of bimolecular reaction kinetics in porous media. Environmental Science & Technology 34 (7), 1234–1239. http://dx.doi.org/10.1021/es9908669.
Rolle, M., Eberhardt, C., Chiogna, G., Cirpka, O.A., Grathwohl, P., 2009. Enhancement of dilution and transverse reactive mixing in porous media: experiments and model-based interpretation. Journal of Contaminant Hydrology 110 (3–4), 130–142. http://dx.doi.org/10.1016/j.jconhyd.2009.10.003.
Saaltink, M.W., Ayora, C., Carrera, J., 1998. A mathematical formulation for reactive transport that eliminates mineral concentrations. Water Resources Research 34 (7), 1649–1656.
Sanchez-Vila, X., Donado, L.D., Guadagnini, A., Carrera, J., 2010. A solution for multicomponent reactive transport under equilibrium and kinetic reactions. Water Resources Research 46 (7), 1–13. http://dx.doi.org/10.1029/2009WR008439.
Steefel, C., Lasaga, A.C., 1994. A coupled model for transport of multiple chemical species and kinetic precipitation/dissolution reactions with application to reactive flow in single phase hydrothermal systems. American Journal of Science 294, 529–592.
Tartakovsky, A.M., Redden, G., Lichtner, P.C., Scheibe, T.D., Meakin, P., 2008. Mixing-induced precipitation: experimental study and multiscale numerical analysis. Water Resources Research 44 (6), 1–19. http://dx.doi.org/10.1029/2006WR005725.
Werth, C.J., Cirpka, O.A., Grathwohl, P., 2006. Enhanced mixing and reaction through flow focusing in heterogeneous porous media. Water Resources Research 42 (12), 1–10. http://dx.doi.org/10.1029/2005WR004511.
Zinn, B., Meigs, L.C., Harvey, C.F., Haggerty, R., Peplinski, W.J., Von Schwerin, C.F., 2004. Experimental visualization of solute transport and mass transfer processes in two-dimensional conductivity fields with connected regions of high conductivity. Environmental Science & Technology 38 (14), 3916–3926.